Bicocca-FT-01-01
GEF/TH-2-01
YITP-SB-01-01
hep-ph/0102134

The $p_{\rm T}$ Spectrum in Heavy-Flavour Photoproduction

Matteo Cacciari[1], Stefano Frixione[2] and Paolo Nason[3]

[1]*C.N. Yang Institute for Theoretical Physics*
State University of New York
Stony Brook, NY 11794-3840

[2]*INFN, Sezione di Genova*
Via Dodecaneso 33, 16146 Genova, Italy

[3]*INFN, Sezione di Milano*
Via Celoria 16, 20133 Milan, Italy

Abstract

We consider the transverse-momentum distribution of heavy flavours in photon-hadron collisions. We present a formalism in which large transverse-momentum logarithms are resummed to the next-to-leading level, and mass effects are included exactly up to order $\alpha_{\rm em}\alpha_{\rm s}^2$, so as to retain predictivity at both small and large transverse momenta. Phenomenological applications relevant to charm photoproduction at HERA are given.

Preprint
January 2001

1 Introduction

This work deals with the computation of the transverse momentum distribution in heavy flavour photoproduction. At present, fixed order (FO) calculations are available, including NLO (Next-to-Leading-Order) corrections [1, 2]. Furthermore, for very large transverse momenta, the so-called fragmentation function (or resummed) formalism, that allows to resum enhanced terms of order $\alpha_{\rm em}\alpha_{\rm s}(\alpha_{\rm s}\log p_{\rm T}/m)^i$ (which we call leading-logarithmic terms, or LL), plus terms of order $\alpha_{\rm em}\alpha_{\rm s}^2(\alpha_{\rm s}\log p_{\rm T}/m)^i$ (next-to-leading logarithmic terms, or NLL) has been developed in ref. [3], building upon ref. [4]. This approach has however the drawback that it is essentially a "massless" formalism, in the sense that it does not include contributions to the cross section that are suppressed by powers of $m/p_{\rm T}$.

Several H1 [5] and ZEUS [6] results are presented in comparison either with calculations performed in the resummed (massless) approach (RS), or with the fixed-order NLO calculation. It is thus important to provide a framework for computing a heavy-flavour cross section which is accurate in both the large and the small transverse momentum regions. A method for performing the merging of the FO [7, 8, 9, 10] and RS [11] calculations in the hadroproduction case was developed in ref. [12]. In the hadroproduction context it was found that the mass corrections are positive and large, a result somewhat contrary to the intuitive belief that masses reduce the phase space, and thus the cross sections.

The aim of the present work is to extend the formalism of ref. [12] to the photoproduction case. This extension is not a straightforward one. In fact, it is well known that a generic photoproduction cross section has to be written as the sum of two components (*pointlike* and *hadronic*, also called *direct* and *resolved* respectively). For the transverse momentum spectrum of a heavy quark we write

$$\frac{d\sigma}{dy\,dp_{\rm T}^2} = \left.\frac{d\sigma}{dy\,dp_{\rm T}^2}\right|_{\rm pnt} + \left.\frac{d\sigma}{dy\,dp_{\rm T}^2}\right|_{\rm hdr}, \tag{1.1}$$

where pnt stands for pointlike and hdr for hadronic; y is the rapidity of the heavy quark in the laboratory frame, and

$$\left.\frac{d\sigma}{dy\,dp_{\rm T}^2}\right|_{\rm pnt} = \sum_j \int dx_{\rm p}\, F_j^{(H)}(x_{\rm p})\, \frac{d\hat{\sigma}_{\gamma j}}{dy\,dp_{\rm T}^2}(P_\gamma, x_{\rm p}P_H), \tag{1.2}$$

$$\left.\frac{d\sigma}{dy\,dp_{\rm T}^2}\right|_{\rm hdr} = \sum_{ij} \int dx_\gamma\, dx_{\rm p}\, F_i^{(\gamma)}(x_\gamma)\, F_j^{(H)}(x_{\rm p})\, \frac{d\hat{\sigma}_{ij}}{dy\,dp_{\rm T}^2}(x_\gamma P_\gamma, x_{\rm p}P_H). \tag{1.3}$$

The sums run over parton flavours, P_γ and P_H are the four-momenta of the incoming photon and hadron respectively, and $d\hat{\sigma}_{\gamma j}$, $d\hat{\sigma}_{ij}$ are the subtracted partonic cross sections. The pointlike and hadronic components of eqs. (1.2) and (1.3) are strictly related beyond the leading order in perturbation theory: none of them is a physical quantity, only their sum (eq. (1.1)) is measurable. This is the origin of the most serious problem we face when extending the formalism of ref. [12] to the present case. In this work we shall follow the strategy adopted in that paper, but we shall point out the major differences with respect to it, due to the problems inherent to eq. (1.1).

In perturbation theory at next-to-leading order (i.e., the highest accuracy reached so far in the computation of heavy flavour cross sections), we have the expansions

$$d\hat{\sigma}_{\gamma j} = \alpha_{\rm em}\alpha_{\rm s} d\hat{\sigma}^{(0)}_{\gamma j} + \alpha_{\rm em}\alpha_{\rm s}^2 d\hat{\sigma}^{(1)}_{\gamma j} \,, \tag{1.4}$$

$$d\hat{\sigma}_{ij} = \alpha_{\rm s}^2 d\hat{\sigma}^{(0)}_{ij} + \alpha_{\rm s}^3 d\hat{\sigma}^{(1)}_{ij} \,. \tag{1.5}$$

However, the parton densities in the photon $F_i^{(\gamma)}$ behave asymptotically (i.e., at large scales) as $\alpha_{\rm em}/\alpha_{\rm s}$. Thus, at least at the formal level, the perturbative expansions of the pointlike and hadronic components of eqs. (1.2) and (1.3) are both series in $\alpha_{\rm em}\alpha_{\rm s}^k$, as in eq. (1.4). This allows us to simplify substantially our presentation; in what follows, we shall write the physical cross section of eq. (1.1) as an expansion in $\alpha_{\rm em}\alpha_{\rm s}^k$. The reader must keep in mind that, in doing this, we are not referring to the pointlike component only, but to the observable that is actually measured in experiments. When we shall deal either with the pointlike or with the hadronic component only, we shall indicate it explicitly.

Having clarified this point, we proceed in our program of extending the formalism of ref. [12] to photoproduction reactions. This means that we shall implement a computation with the following features:

- All terms of order $\alpha_{\rm em}\alpha_{\rm s}$ and $\alpha_{\rm em}\alpha_{\rm s}^2$ are included exactly, including mass effects;
- All terms of order $\alpha_{\rm em}\alpha_{\rm s}\left(\alpha_{\rm s}\log p_{\rm T}/m\right)^i$ and $\alpha_{\rm em}\alpha_{\rm s}^2\left(\alpha_{\rm s}\log p_{\rm T}/m\right)^i$ are included, with the possible exception of terms that are suppressed by powers of $m/p_{\rm T}$.

To be more specific, let us write schematically the result of the NLO calculation of the photoproduction cross section as

$$\frac{d\sigma}{dy\,dp_{\rm T}^2} = A(m)\alpha_{\rm em}\alpha_{\rm s} + B(m)\alpha_{\rm em}\alpha_{\rm s}^2 + \mathcal{O}(\alpha_{\rm em}\alpha_{\rm s}^3) \,. \tag{1.6}$$

The explicit dependence of A and B upon $E_{\rm cm}$ (the centre-of-mass energy), y, $p_{\rm T}$ and the factorization/renormalization scale μ is not indicated, and $\alpha_{\rm s} = \alpha_{\rm s}(\mu)$. The NLL resummed cross section is given by

$$\begin{aligned}\frac{d\sigma}{dy\,dp_{\rm T}^2} &= \alpha_{\rm em}\alpha_{\rm s}\sum_{i=0}^{\infty} a_i(\alpha_{\rm s}\log\mu/m)^i + \alpha_{\rm em}\alpha_{\rm s}^2\sum_{i=0}^{\infty} b_i(\alpha_{\rm s}\log\mu/m)^i \\ &\quad +\mathcal{O}(\alpha_{\rm em}\alpha_{\rm s}^3(\alpha_{\rm s}\log\mu/m)^i) + \mathcal{O}(\alpha_{\rm em}\alpha_{\rm s}\times{\rm PST})\,, \end{aligned} \tag{1.7}$$

where PST stands for terms suppressed by powers of $m/p_{\rm T}$ in the large-$p_{\rm T}$ limit (possibly with further powers of mass logarithms). The coefficients a_i and b_i depend upon $E_{\rm cm}$, y, $p_{\rm T}$ and μ. If $\mu \approx p_{\rm T}$, they do not contain large logarithms of the order of $\log p_{\rm T}/m$. The only large logarithms are the ones explicitly indicated. Our approach combines the results of eqs. (1.6) and (1.7), giving

$$\begin{aligned}\frac{d\sigma}{dy\,dp_{\rm T}^2} &= A(m)\alpha_{\rm em}\alpha_{\rm s} + B(m)\alpha_{\rm em}\alpha_{\rm s}^2 + \\ &\quad \left(\alpha_{\rm em}\alpha_{\rm s}\sum_{i=2}^{\infty} a_i(\alpha_{\rm s}\log\mu/m)^i + \alpha_{\rm em}\alpha_{\rm s}^2\sum_{i=1}^{\infty} b_i(\alpha_{\rm s}\log\mu/m)^i\right)\times G(m,p_{\rm T}) \\ &\quad +\mathcal{O}(\alpha_{\rm em}\alpha_{\rm s}^3(\alpha_{\rm s}\log\mu/m)^i) + \mathcal{O}(\alpha_{\rm em}\alpha_{\rm s}^3\times{\rm PST})\,, \end{aligned} \tag{1.8}$$

where the function $G(m,p_{\rm T})$ is quite arbitrary, except that it must be a smooth function (also in the $p_{\rm T}\to 0$ limit), and that it must approach one when $m/p_{\rm T}\to 0$, up to terms suppressed by powers of $m/p_{\rm T}$. Observe that the sums now start from $i=2$ and $i=1$, respectively, in order to avoid double counting. Thus, this formalism contains all the information coming from the fixed-order NLO calculation *and* from the NLL resummed calculation. The arbitrariness in the function G arises from the fact that we do not know the structure of power-suppressed terms in the higher orders of the NLL resummed calculation. The choice of the function G only affects terms of order $\alpha_{\rm em}\alpha_{\rm s}^3$, so far unknown.

Before turning to the practical implementation of eq. (1.8), we stress that it is important that both the RS and the FO approaches are expressed in the same renormalization scheme. The commonly used FO approach uses a renormalization and factorization scheme in which the heavy flavour is treated as heavy. Thus, if we are dealing with charm, we use $\alpha_{\rm s}$ of 3 light flavours as our running coupling constant, and the appropriate structure functions should not include the charm quark in the evolution. The RS approach, on the other hand, also includes the heavy flavour as

an active, light degree of freedom. This problem can be easily overcome by a simple change of scheme in the FO calculation. Section 2 contains the details of this procedure.

Once this is done, the FO calculation matches exactly the terms up to order $\alpha_{\rm em}\alpha_{\rm s}^2$ in the resummed approach, in the limit where power-suppressed mass terms are negligible. In order to subtract from the RS result the terms already present in the FO, we must provide an approximation to the latter where terms suppressed by powers of the mass are dropped. We shall call FOM0 this "massless limit". In the simplified notation of eqs. (1.6) and (1.7) we have

$$A(m) = a_0 + \mathrm{PST}\,, \quad B(m) = a_1 \log \mu/m + b_0 + \mathrm{PST}\,, \tag{1.9}$$

and the FOM0 approximation is given by

$$\left.\frac{d\sigma}{dy\,dp_{\rm T}^2}\right|_{\rm FOM0} = a_0\alpha_{\rm em}\alpha_{\rm s} + (a_1 \log \mu/m + b_0)\,\alpha_{\rm em}\alpha_{\rm s}^2\,. \tag{1.10}$$

Our final result will be given by

$$\mathrm{FONLL} = \mathrm{FO}\ + (\mathrm{RS}\ -\ \mathrm{FOM0})\ \times G(m, p_{\rm T})\,. \tag{1.11}$$

The notation FONLL stands for fixed-order plus next-to-leading logs. Formula (1.11) is our practical implementation of eq. (1.8).

The quantities appearing in the RHS of eq. (1.11) are available as Fortran computer codes. Actually, due to the non-physical splitting of photoproduction cross sections as given in eq. (1.1), the pointlike and hadronic components are usually computed by different packages. It is therefore useful to write

$$\mathrm{FO} = \mathrm{FO}_{\rm pnt} + \mathrm{FO}_{\rm hdr}, \quad \mathrm{FOM0} = \mathrm{FOM0}_{\rm pnt} + \mathrm{FOM0}_{\rm hdr}, \quad \mathrm{RS} = \mathrm{RS}_{\rm pnt} + \mathrm{RS}_{\rm hdr}. \tag{1.12}$$

The package that computes $\mathrm{FO}_{\rm hdr}$ was originally developed in ref. [8], and subsequently modified in ref. [12], in order to implement $\mathrm{FOM0}_{\rm hdr}$ (whose analytical form was obtained in ref. [8]), and in order to use the appropriate renormalization and factorization scheme. $\mathrm{FO}_{\rm pnt}$ was computed in refs. [1] and [2], and $\mathrm{FOM0}_{\rm pnt}$ was obtained in the present work. The code for $\mathrm{FO}_{\rm pnt}$ (taken from ref. [1]) has been extensively modified in the context of the present work in a manner analogous to what done for $\mathrm{FO}_{\rm hdr}$ in ref. [12]. The package that computes $\mathrm{RS}_{\rm hdr}$ was presented in ref. [13], suitably modified for heavy quark fragmentation in ref. [11], and used in

ref. [12]. Finally, the package relevant to $\mathrm{RS_{pnt}}$ was written by the authors of ref. [14], and adapted to heavy quark fragmentation in ref. [3]. It has undergone some further modifications during the course of this work. It should be clear that FO, FOM0, and RS are all strictly interrelated. This fact provides us with a way not only to test that the various codes mentioned above are mutually consistent, but also that their implementation in our formalism, eq. (1.8), has been carried out correctly. In particular, the relation between FO and FOM0, and between FOM0 and RS, will be the argument of sections 3 and 4 respectively. In the latter section, we shall show in particular that the FOM0 and RS results differ only by terms of order $\alpha_{\mathrm{em}}\alpha_{\mathrm{s}}^3$.

The paper is organized as follows. In sect. 2 we describe the procedure to adopt in order to translate the FO result from a scheme with $n_{\mathrm{f}}-1$ light flavours to a scheme with n_{f} light flavours. In sect. 3 we give a few details concerning the calculation of the massless limit of the FO calculation. In sect. 4 we check the matching between the FOM0 and the RS calculation. Unlike in the hadroproduction case, subtleties arise here due to a different separation of the hadronic and pointlike contributions in the FO and RS approaches. We shall see that only in the full (i.e. pointlike plus hadronic) cross section we have complete matching. In sect. 5 we examine the size of power-suppressed effects in order to understand at which value of m/p_{T} the massless approach gives a sensible approximation to the massive calculation. The function $G(m,p_{\mathrm{T}})$ will be chosen on the basis of the considerations given in this section. In sect. 6 we describe our full result, for the case of charm production at HERA. Finally, in sect. 7 we give our conclusions.

2 The change of scheme

As shown in detail in ref. [12], a change of scheme from the one with n_{lf} to the one with $n_{\mathrm{f}}=n_{\mathrm{lf}}+1$ light flavours brings about the following changes in α_{s} and in the parton densities

$$\alpha_{\mathrm{s}}^{(n_{\mathrm{lf}})}(\mu_{\mathrm{R}}) = \alpha_{\mathrm{s}}^{(n_{\mathrm{f}})}(\mu_{\mathrm{R}}) - \frac{1}{3\pi}T_{\mathrm{F}}\log\frac{\mu_{\mathrm{R}}^2}{m^2}{\alpha_{\mathrm{s}}^{(n_{\mathrm{f}})}}^2(\mu_{\mathrm{R}}) + \mathcal{O}(\alpha_{\mathrm{s}}^3)\,, \tag{2.1}$$

$$F_g^{(n_{\mathrm{lf}})}(\mu_{\mathrm{F}}) = F_g^{(n_{\mathrm{f}})}(\mu_{\mathrm{F}})\left[1+\frac{\alpha_{\mathrm{s}}^{(n_{\mathrm{f}})}(\mu_{\mathrm{R}})T_{\mathrm{F}}}{3\pi}\log\frac{\mu_{\mathrm{F}}^2}{m^2}\right] + \mathcal{O}(\alpha_{\mathrm{s}}^2). \tag{2.2}$$

All other parton densities are affected at higher orders in α_{s}. Eqs. (2.1) and (2.2) are universal, that is, process-independent. It is easy to convince oneself that the

pointlike and hadronic components of the cross sections transform independently under this change of scheme. Thus, for what concerns the latter component, we can safely use the formulae of ref. [12]. In the pointlike component, the only effect at $\mathcal{O}(\alpha_{\rm em}\alpha_{\rm s}^2)$ is generated by the Born-level γg cross section. It is a matter of trivial algebra to conclude that, in order to go from the $n_{\rm lf}$-flavour to the $n_{\rm f}$-flavour scheme, the fixed-order cross section has to be modified by adding a term

$$\delta\sigma_{\gamma g} = -\alpha_{\rm s}\frac{1}{3\pi}T_{\rm F}\log\frac{\mu_{\rm R}^2}{\mu_{\rm F}^2}\,\sigma_{\gamma g}^{(0)} \tag{2.3}$$

to the γg cross section. For any reasonable range of scales, this correction is not large, and it vanishes for $\mu_{\rm F} = \mu_{\rm R}$.

In the following, we shall always refer to the FO and FOM0 calculations performed in the $n_{\rm f}$-flavour scheme. We shall thus always assume that $\alpha_{\rm s}$ and the parton densities F_j refer to $\alpha_{\rm s}^{(n_{\rm f})}$ and $F_j^{(n_{\rm f})}$.

3 Massless limit of the fixed-order calculation

As in the case of the change of scheme, the massless limit of FO can clearly be performed independently for the pointlike and hadronic components. The latter has been considered in ref. [12]; here, we only deal with the pointlike part.

The massless limit of the fixed-order pointlike cross section formulae (in the sense of eq. (1.10)) is obtained via algebraic methods from the results of ref. [1]. As pointed out in ref. [8], the limiting procedure is non-trivial. In fact, the partonic cross sections at order $\alpha_{\rm em}\alpha_{\rm s}^2$ contain distributions, such as delta functions or principal value singularities. When taking the massless limit, new contributions to these distributions arise. We have computed this limit analytically by a computer-algebra procedure applied to the massive cross section formula, and checked its correctness in the following way. We compute the heavy-flavour differential cross section at fixed $p_{\rm T}$, y, and centre-of-mass energy. We choose the renormalization and factorization scales equal to $p_{\rm T}$. Under these conditions, the mass dependence of the result is confined to the partonic cross sections. In the massless limit approximation, the only remnants of mass dependence are in logarithms of the mass in the $\mathcal{O}(\alpha_{\rm em}\alpha_{\rm s}^2)$ terms. Thus, if we plot the $\text{FOM0}_{\rm pnt}$ cross section versus the logarithm of the mass, we get a straight line. On the other hand, if we plot the full $\text{FO}_{\rm pnt}$ cross section versus the logarithm of the mass, it should approach the $\text{FOM0}_{\rm pnt}$ result in the limit of small masses. We

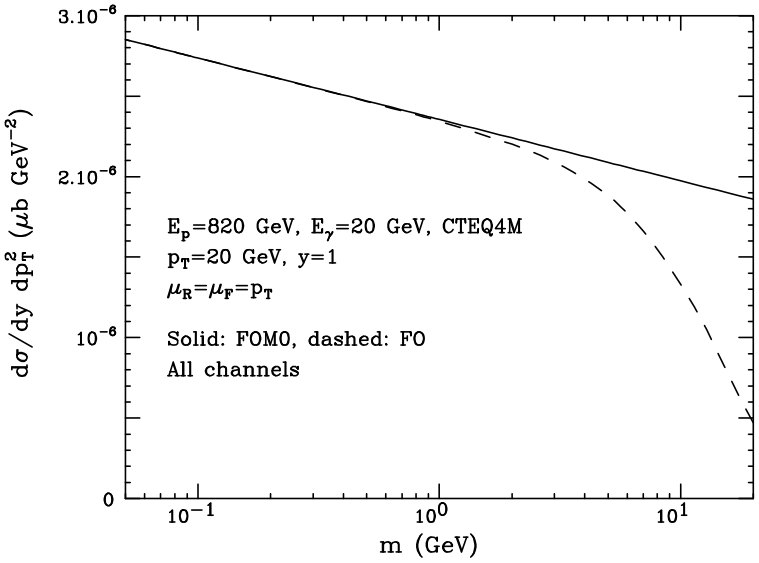

Figure 1: Comparison of the $\mathrm{FO}_{\mathrm{pnt}}$ and $\mathrm{FOM0}_{\mathrm{pnt}}$ differential cross sections as a function of the logarithm of the mass, at $p_{\mathrm{T}} = 20$ GeV and $y = 1$.

have performed this test, choosing the proton energy $E_{\mathrm{p}} = 820$ GeV and the photon energy $E_\gamma = 20$ GeV. We adopt the CTEQ4M set [15] for the proton parton density functions. These parameters will be our reference choice from now on. The results are displayed in figs. 1 and 2. From the figures, it is quite apparent that the massless limit, as well as its implementation for the calculation of cross sections, was carried out correctly. There is also an important observation to make: the $\mathrm{FOM0}_{\mathrm{pnt}}$ cross section is *larger* than the massive calculation, i.e. power suppressed mass effects are negative, contrary to the case of hadroproduction.

Notice also that the $\mathrm{FOM0}_{\mathrm{pnt}}$ approximation is quite accurate even at relatively large values of m/p_{T}. For example, from both figs. 1 and 2 we notice that even for $m/p_{\mathrm{T}} \approx 1/2$, the $\mathrm{FO}_{\mathrm{pnt}}$ cross section differs from $\mathrm{FOM0}_{\mathrm{pnt}}$ by at most 30%. This has to be contrasted with the case of the hadronic component (see ref. [12]), where $\mathrm{FOM0}_{\mathrm{hdr}}$ is describing well $\mathrm{FO}_{\mathrm{hdr}}$ only for rather small values of m/p_{T}. This mismatch between the behaviour of the pointlike and the hadronic component will clearly show up in phenomenologically relevant cases, as we shall later see in sect. 6.

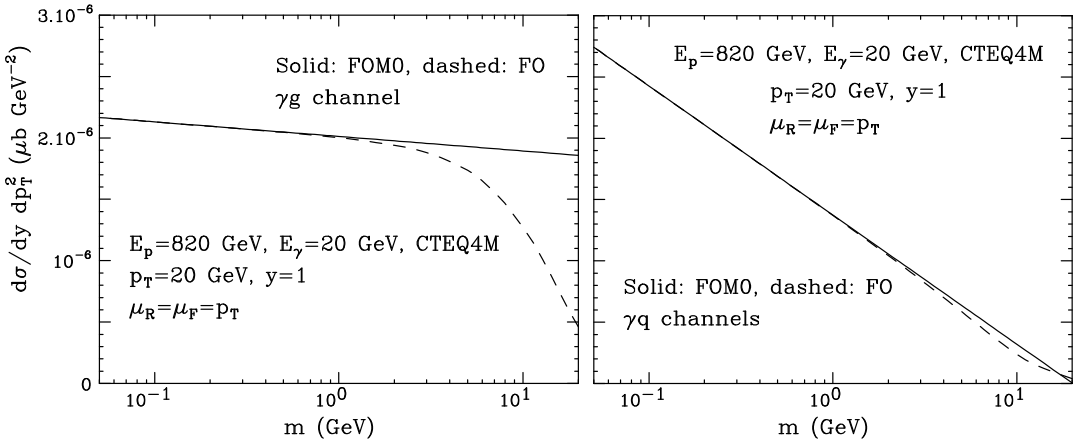

Figure 2: As in figure 1, for γg (left) and γq (right) components alone.

4 Matching

We now examine the matching between the resummed approach and the FOM0 calculation. In this case, there is a strict interplay between the pointlike and the hadronic components, that should be dealt with very carefully.

There are ingredients in the resummed approach that are not explicitly present in the FOM0 calculation. These are the fragmentation functions for final-state partons to go into the heavy quark, and the parton density for finding a heavy quark inside the hadron. The fragmentation function for any parton to go into a heavy quark has a power expansion in terms of the coupling constant evaluated at the scale μ[1], and of logarithms of μ/m:

$$D_j(x,\mu,m) = \sum_{k=0}^{\infty} \sum_{l=0}^{k} d_j^{(k,l)}(x)\, \log^l \frac{\mu}{m}\, \alpha_{\rm s}^k(\mu)\,, \tag{4.1}$$

that can be obtained by solving the evolution equation for the fragmentation function at the NLL level, with the initial conditions of ref. [4]. Similarly, the parton density for finding the heavy flavour in a hadron can be expanded in the form

$$F_h(x,\mu,m) = \sum_{k=0}^{\infty} \sum_{l=0}^{k} f^{(k,l)}(x, F_l(\mu)) \log^l \frac{\mu}{m}\, \alpha_{\rm s}^k(\mu)\,. \tag{4.2}$$

With $F_l(\mu)$ in the argument of the coefficients, we mean that the coefficients have a complicated *functional* dependence upon the parton densities evaluated at the scale

[1] We take for simplicity $\mu_{\rm R} = \mu_{\rm F} = p_{\rm T}$, and denote the common value with μ.

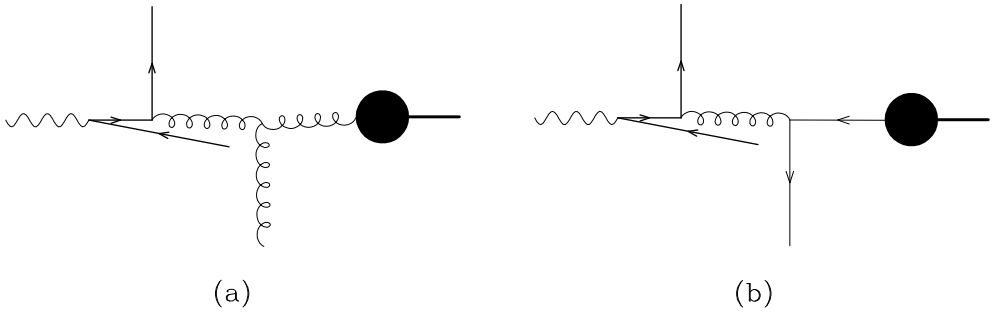

Figure 3: Photon splitting into a heavy-quark pair.

μ. The existence of formal expansions of the form (4.1) and (4.2) can be easily proved, by writing the Altarelli–Parisi equations in integral form, and then solving them iteratively. A more detailed argument was given in Appendix A of ref. [12].

Once eqs. (4.1) and (4.2) are formally substituted in the RS cross section formula, this formula itself becomes a power expansion of the form of eq. (1.7), with the coefficients that depend (functionally) upon the structure functions for light partons, in the $n_{\rm f}$-flavours scheme, evaluated at the scale μ. The FOM0 calculation has an expansion of the same form (truncated to order $\alpha_{\rm em}\alpha_{\rm s}^2$) with coefficients that are also dependent upon the same light-parton structure functions[2] evaluated at the scale μ. Thus, because of the next-to-leading logarithmic accuracy of the resummed cross section, the terms up to the order $\alpha_{\rm em}\alpha_{\rm s}^2$ in RS will match exactly with the FOM0 calculation.

In the photoproduction case, the matching can take place only in the full cross section, i.e. pointlike plus hadronic. In fact, let us consider the photoproduction subprocess in which a photon splits into a heavy-quark pair, and afterwards the heavy quark scatters with a parton coming from the hadron, as shown in fig. 3. The contributions depicted in the figure, in the kinematic region of a photon splitting collinearly, is fully included in the pointlike contribution in the massive, fixed order calculation. In fact, because of the mass, no collinear subtractions are needed on the photon side.

In the resummed approach, instead, these graphs are collinear divergent, and the

[2]We observe that this property of the FOM0 calculation is only valid in the modified scheme described in section 2. If we had used the standard scheme for the fixed-order calculation, the structure functions and the coupling $\alpha_{\rm s}$ appearing there would be those with $n_{\rm f}-1$ flavours.

singularities are subtracted at a scale μ. A corresponding hadronic contribution is present, where a heavy quark is found inside the incoming photon. Such a contribution is not present in the hadronic part of the fixed-order approach.

Therefore, in order to check the matching, we should consider pointlike plus hadronic cross sections, and compute the difference between two relatively large numbers (RS and FOM0), each of which is obtained as the sum of two numbers ($\mathrm{RS_{pnt}}$ plus $\mathrm{RS_{hdr}}$ and $\mathrm{FOM0_{pnt}}$ plus $\mathrm{FOM0_{hdr}}$). In practice, this procedure requires an extremely careful treatment of numerics, which is not required anywhere else in our study. We thus adopted a slightly different, although equivalent, strategy, which is based upon the observation that, as far as the matching is concerned, it is only the contribution depicted in fig. 3 that is treated differently in RS and FOM0. Therefore, we can simply add to the resummed pointlike result the hadronic contribution with a heavy quark in a photon. Since the matching is checked up to the order $\alpha_{\mathrm{em}}\alpha_{\mathrm{s}}^2$, it is enough to compute such contribution at this order. Calling s the s-channel invariant of the photon-hadron system and y_h (y_l) the heavy quark (light recoiling parton) rapidity in the photon-hadron CM system, we immediately find

$$\frac{d\hat{\sigma}_{\mathrm{PQ}}}{dy_h dp_{\mathrm{T}}^2} = \int \frac{1}{8\pi s} \sum_l P_{h\gamma}(x_\gamma) \log\frac{\mu_{\mathrm{F}}^2}{m^2}\, F_l^{(p)}(x_{\mathrm{p}},\mu_{\mathrm{F}}) \frac{d\hat{\sigma}_{hl}^{(0)}(p_{\mathrm{T}},\hat{y})}{d\Phi_2}\, dy_l \tag{4.3}$$

where PQ stands for photon to quark, and

$$P_{h\gamma}(x) = \frac{\alpha_{\mathrm{em}}}{2\pi} N_c e_h^2 (x^2 + (1-x)^2)\ . \tag{4.4}$$

$d\hat{\sigma}_{hl}^{(0)}/d\Phi_2$ is the leading order (i.e. $\mathcal{O}(\alpha_{\mathrm{s}}^2)$) massless cross section (without the two-body phase space) for the partons h (the heavy quark) and l (a light quark or a gluon) to give an outgoing heavy quark h with transverse momentum p_{T} and rapidity $\hat{y}$ in the parton centre-of mass (CM). The variables p_{T} and $\hat{y}$ characterize completely the scattering kinematics in the partonic CM system. We have furthermore

$$\hat{y} = \frac{y_h - y_l}{2}\,, \tag{4.5}$$

$$x_\gamma = \sqrt{\frac{4p_{\mathrm{T}}^2}{s}}\,\frac{\exp(y_h)+\exp(y_l)}{2}\,, \tag{4.6}$$

$$x_{\mathrm{p}} = \sqrt{\frac{4p_{\mathrm{T}}^2}{s}}\,\frac{\exp(-y_h)+\exp(-y_l)}{2} \tag{4.7}$$

and the partonic cross sections are

$$\frac{d\hat{\sigma}_{hq}^{(0)}(p_{\mathrm{T}},\hat{y})}{d\Phi_2} = (4\pi\alpha_{\mathrm{s}})^2\,\frac{1}{2\hat{s}}\,\frac{4}{9}\,\frac{\hat{s}^2+\hat{u}^2}{\hat{t}^2}\,, \tag{4.8}$$

$$\frac{d\hat{\sigma}^{(0)}_{hg}(p_{\rm T},\hat{y})}{d\Phi_2} = (4\pi\alpha_{\rm s})^2\,\frac{1}{2\hat{s}}\left(-\frac{4}{9}\frac{\hat{s}^2+\hat{u}^2}{\hat{s}\hat{u}}+\frac{\hat{u}^2+\hat{s}^2}{\hat{t}^2}\right), \tag{4.9}$$

where the partonic Mandelstam variables $\hat{s}$, $\hat{t}$ and $\hat{u}$ are easily obtained from $p_{\rm T}$ and y. For future reference, we shall call PQ (for Photon to Quark) the contribution of eq. (4.3). Such contribution is part of the direct component of the FOM0 result.

In order to check the matching of the resummed and fixed order calculation we proceeded in the following way:

(a) we computed the $\mathrm{FOM0_{pnt}}$ result in the $n_{\rm f}$ flavours scheme;

(b) we computed the RS result without the intrinsic heavy quark component in the hadron parton densities, and with a heavy quark fragmentation function set equal to $\delta(1-z)$ for the D_q component, and all other components set to zero;

(c) we computed the LO contribution to the RS result, with the heavy quark component in the hadron parton densities set equal to

$$F_h^{(H)}(x,\mu) = \frac{\alpha_{\rm s}(\mu)\log\mu^2/m^2}{2\pi}\int_x^1 F_g^{(H)}(x/z,\mu)P_{hg}(z)\frac{dz}{z}, \tag{4.10}$$

and all other components set to zero;

(d) we computed the LO contribution to the RS result, with the heavy quark density set to zero, and the heavy quark fragmentation function set to its $\mathcal{O}(\alpha_{\rm s})$ value

$$D_h(z,\mu) \to \frac{\alpha_s(\mu)C_{\rm F}}{2\pi}\left[\frac{1+z^2}{1-z}\left(\log\frac{\mu^2}{m^2}-2\log(1-z)-1\right)\right]_+ \tag{4.11}$$

$$D_g(z,\mu) \to \frac{\alpha_s(\mu)T_{\rm F}}{2\pi}(z^2+(1-z)^2)\log\frac{\mu^2}{m^2} \tag{4.12}$$

$$D_i(z,\mu) \to 0\,, \quad \text{for } i\neq g,h\,. \tag{4.13}$$

We then verified that the sum of items (b), (c) and (d), plus the PQ contribution (eq. (4.3)) is exactly equal to item (a). Observe that with this procedure we were able to isolate the terms of order $\alpha_{\rm em}\alpha_{\rm s}$ and $\alpha_{\rm em}\alpha_{\rm s}^2$ in the RS result, and thus, in order to check the matching, we did not need to go to the weak coupling limit, as was done in ref. [12]. The resummed hadronic component, suitably augmented of the PQ contribution, must then match the fixed order hadronic component in the massless limit. This follows easily from the work of ref. [12].

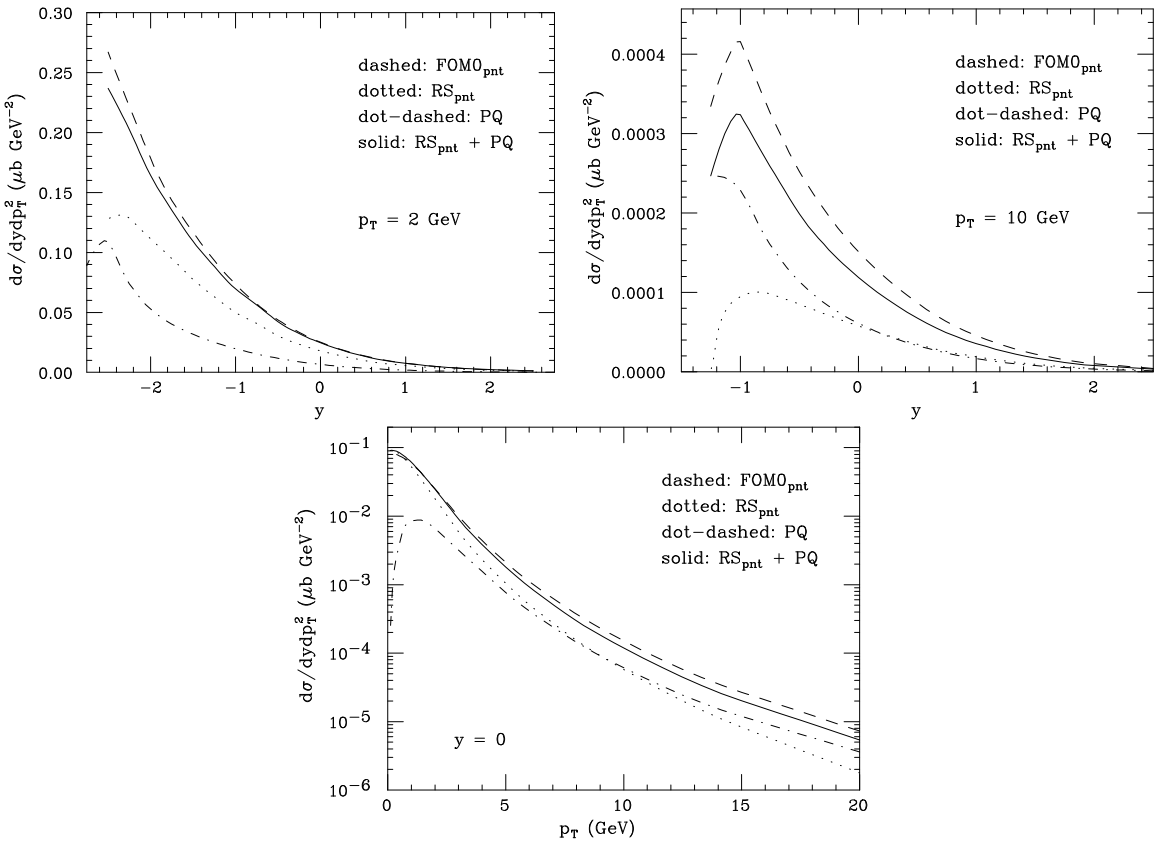

Figure 4: $\mathrm{FOM0_{pnt}}$ compared to the sum of $\mathrm{RS_{pnt}}$ and PQ. The parameters are as in fig. 1. The charm quark mass was set equal to 1.5 GeV.

The procedure we carried out, besides convincing us of the correctness of our theoretical approach, has also served as a test of consistency between the computer programs of ref. [14] and the fixed order calculation of ref. [1].

We have thus demonstrated that the quantity $\mathrm{RS_{pnt}} + \mathrm{PQ} - \mathrm{FOM0_{pnt}}$ is of order $\alpha_{\mathrm{em}}\alpha_{\mathrm{s}}^3$. However, this does *not* guarantee that it is also small in practice. In ref. [12] it was shown[3] that $\mathrm{RS} - \mathrm{FOM0}$ in the case of hadronic collisions is of order α_{s}^4, but it is numerically non-negligible even for bottom production. We shall now show that, in the present case, the difference $\mathrm{RS_{pnt}} + \mathrm{PQ} - \mathrm{FOM0_{pnt}}$ is numerically small, at least in the region where $\alpha_{\mathrm{s}} \log p_{\mathrm{T}}/m$ is also small (that is to say when p_{T} is not large). This is in fact what we see in fig. 4. We also see that, as previously discussed, $\mathrm{FOM0_{pnt}}$ is not a good approximation of $\mathrm{RS_{pnt}}$, due to the lack of the photon-splitting term

[3]See in particular fig. 8 of ref. [12]

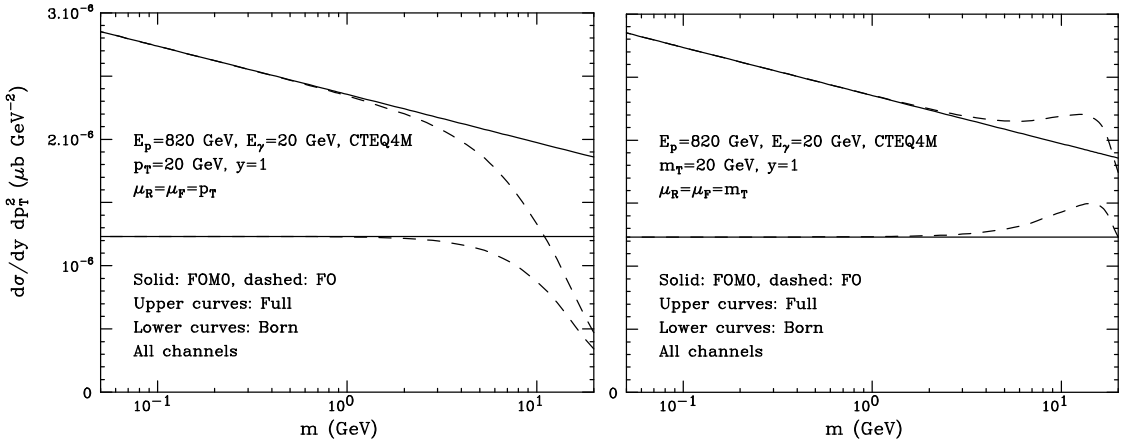

Figure 5: $\mathrm{FO}_{\mathrm{pnt}}$ and $\mathrm{FOM0}_{\mathrm{pnt}}$ at Born and full $\mathcal{O}(\alpha_{\mathrm{em}}\alpha_{\mathrm{s}}^2)$ level, plotted as a function of the mass and at fixed transverse momentum (left figure) or fixed transverse mass (right figure).

PQ. We further note that the matching deteriorates at higher values of p_{T}, due to the increasing importance of the resummation performed in $\mathrm{RS}_{\mathrm{pnt}}$ but absent in $\mathrm{FOM0}_{\mathrm{pnt}}$.

5 Power effects in the RS and FOM0 calculations

When comparing and matching the FO, FOM0 and RS approaches, there is much arbitrariness in the way mass effects are treated. For example, we may decide to compare transverse-mass distributions instead of transverse momenta. These are equal for the FOM0 and RS calculations, but differ in the FO case. In ref. [12] the effect of this replacement was studied for hadron-hadron cross sections. Here we thus study only the pointlike component $\mathrm{FO}_{\mathrm{pnt}}$ and $\mathrm{FOM0}_{\mathrm{pnt}}$.

In fig. 5 we plot $\mathrm{FO}_{\mathrm{pnt}}$ and $\mathrm{FOM0}_{\mathrm{pnt}}$ as a function of the mass, keeping either m_{T} or p_{T} fixed. It is clear that, in the plots at fixed transverse momentum, the massive calculation is more suppressed near the threshold (i.e., as m approaches p_{T}). In this region higher x_{p} values are probed in the proton structure function with respect to the massless calculation since, besides the transverse momentum, also the mass has to be produced. This is clearly a spurious effect, and we shall always prefer to perform the matching at fixed transverse masses. The right plot of fig. 5 is an *a posteriori* justification of this procedure, since it is quite clear that in this case the massive and massless limit results are much closer to each other. It is also worth noting that in the

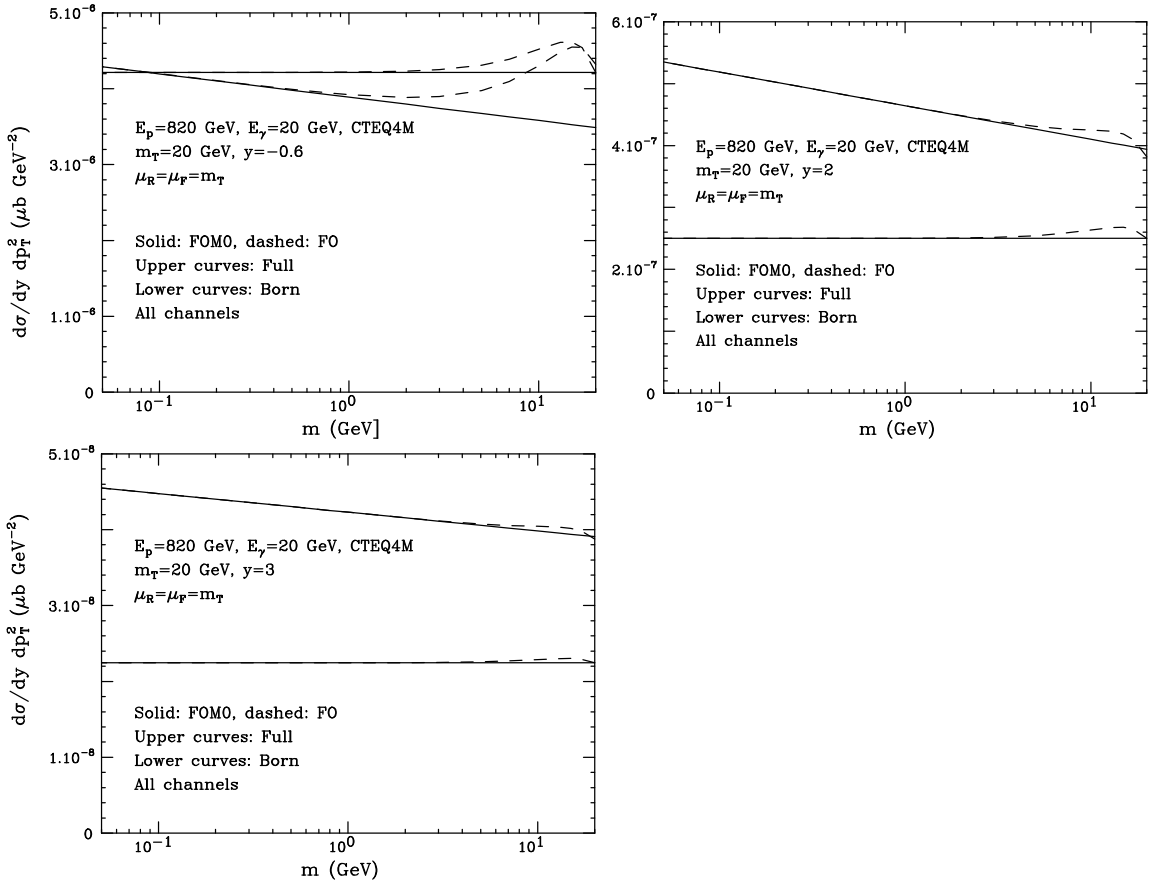

Figure 6: As in the right plot of fig. 5, for $y = -0.6$, 2 and 3.

right plot of fig. 5 power suppressed mass effects are positive, in contrast to what we observed earlier (see fig. 1). In figure 6 we show analogous plots at fixed transverse mass for $y = -0.6$, 2 and 3. In all cases the massless limit and full massive results are in good agreement, although a worsening is seen for the case of $y = -0.6$. This rapidity value is quite close to the phase space boundary, where we do in fact expect some anomalous behaviour due to Sudakov logarithms.

We shall now proceed as follows. For a given transverse momentum $p_{\rm T}$, the FO cross section is evaluated and combined, using eq. (1.11), with the FOM0 and RS results evaluated at the corresponding $m_{\rm T} = \sqrt{p_{\rm T}^2 + m^2}$ value. In this way the three calculations are performed at the same $m_{\rm T}$. Moreover, a central choice for the renormalization and factorization scales will be $\mu_{\rm R} = \mu_{\rm F} = \sqrt{p_{\rm T}^2 + m^2}$, so that they coincide in the three calculations.

In the hadroproduction case [12], a suppression factor $G(m, p_{\rm T})$ was introduced to multiply the RS $-$ FOM0 term in eq. (1.11), with $G(m, p_{\rm T})$ approaching one at large $p_{\rm T}$. The following form was chosen:

$$G(m, p_{\rm T}) = \frac{p_{\rm T}^2}{p_{\rm T}^2 + c^2 m^2} \ . \tag{5.1}$$

Adopting the same form, our final formula becomes

$$\text{FONLL} = \text{FO} \ + \ \frac{p_{\rm T}^2}{p_{\rm T}^2 + c^2 m^2} [\text{RS} \ - \ \text{FOM0}] \ . \tag{5.2}$$

In ref. [12] $c = 5$ was chosen, in order to suppress meaningless large corrections coming from the massless approach at low momenta. A detailed discussion of the role of c in the present case will be given in the next section.

6 Phenomenological results

We now present some benchmark results of our calculation, based upon eq. (5.2). In order to perform the calculation, we have suitably modified the codes relevant to $\text{FO}_{\rm pnt}$, $\text{FOM0}_{\rm pnt}$, and $\text{RS}_{\rm pnt}$, in order to obtain a consistent implementation. The hadronic quantities, on the other hand, have been produced with the program of ref. [12], here modified in order to allow the use of the photon parton densities.

When applying our matched formalism to phenomenology, we must first make sure that the parton densities we use correctly incorporate the logarithms of m/μ that we are trying to resum. This must be the case if the structure functions have been evolved correctly, with the heavy flavour evolution turned on when $\mu = m$, as appropriate in the $\overline{\rm MS}$ scheme [16]. In the structure function fits available today this is not always the case. In part this is due to the fact that the parton densities are often given as an interpolating grid, and the region near the heavy flavour threshold may not be represented accurately. Furthermore some parton density sets do not implement the heavy flavour thresholds according to ref. [16]. While for hadron structure functions several sets with a correct charm density are available, the choice among photon structure functions is quite limited. We have chosen the AFG set [17], which is in the $\overline{\rm MS}$ scheme, and claims a correct implementation of the charm density. In order to test this fact, we have plotted in fig. 7 the AFG charm parton density in

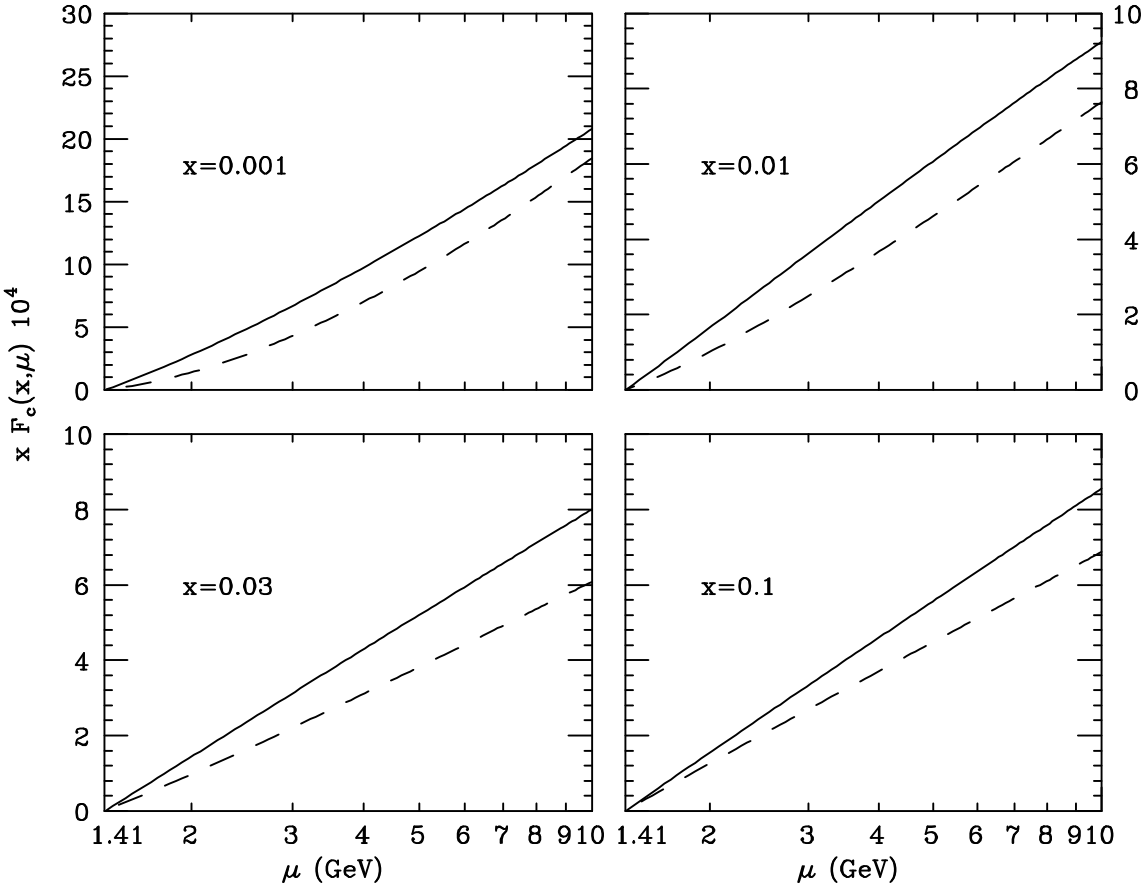

Figure 7: Charm parton density according to the AFG parametrization (solid), compared to eq. (6.1) (dashed).

the photon together with a charm density computed with the following formula:

$$F_c(x,\mu_{\rm F}) = \left[\frac{\alpha_{\rm em}N_c}{2\pi}\,c_c^2(x^2+(1-x)^2) + \frac{\alpha_{\rm s}(\mu_{\rm F})T_{\rm F}}{2\pi}\int_x^1 (z^2+(1-z)^2)F_g(x/z)\frac{dz}{z}\right]\log\frac{\mu_{\rm F}^2}{m^2}\ , \tag{6.1}$$

(where $c_c = 2/3$ is the electric charge of the charm quark) that should hold for factorization scales not too far from the heavy quark mass. In order to match the AFG parameters, we have chosen $m = 1.41$ GeV in this plot. We expect that the slope of the AFG charm density and our approximate formula should agree for small scales. Unfortunately we do not observe this, especially at small values of x. We have checked, however, that these differences would only be marginally important if our approximate formula, eq. (6.1), were used to calculate physical cross sections, the results obtained with the original AFG charm densities being well reproduced.

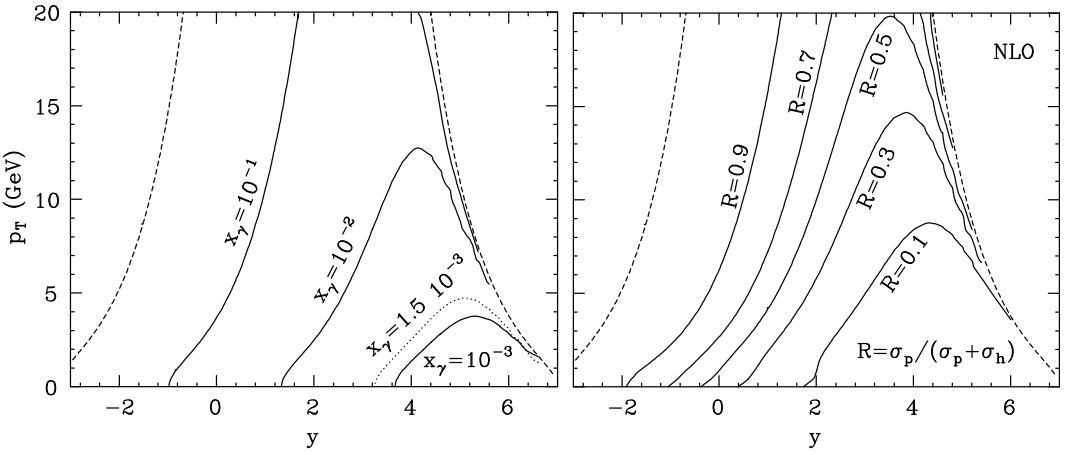

Figure 8: Contours in the y-p_T plane of constant minimum x_γ value probed in the hadronic component (on the left), and of constant ratio of the direct component over the total cross section (on the right) for the NLO result. The short–dashed line represents the phase space boundary.

In what follows, we consider our reference case of photon-proton collisions, with $E_\gamma = 20$ GeV and $E_p = 820$ GeV. In the left panel of fig. 8 we plot contour lines representing the minimum value of x_γ allowed in the hadronic component of the cross section, in the y-p_T plane. Commonly available photon structure function fits are undefined below values of x_γ of the order of 10^{-3}. The minimum value of $x_\gamma = 1.5\ 10^{-3}$ relevant to the AFG set is explicitly shown in the figure. For rapidities currently probed at HERA, smaller x_γ values are never reached. In the right panel of fig. 8 we show, for future reference, the ratio R of the pointlike component over the total cross section, both computed at the NLO. Where the hadronic component prevails (i.e. R becomes small), we expect to find the same problems found in ref. [12] as far as the matching between RS and FOM0 is concerned. We point out that the results displayed in the right panel of fig. 8 have a scale dependence of $\mathcal{O}(\alpha_{\rm em}\alpha_{\rm s}^2)$, and they are thus accurate to LO only; however, the plot gives a clear idea on the dominance of pointlike or hadronic components in the physical cross sections.

In our phenomenological study we shall use $m = 1.5$ GeV, the AFG set for the photon and CTEQ4M for the proton parton densities. In fig. 9 we show the rapidity distribution for charm quarks at $p_T = 2$ GeV. In the left plot of this figure, both the fixed order prediction and our FONLL results are shown. The photon has negative rapidity in our convention. The phase space limit for the rapidity at $p_T = 2$ GeV is

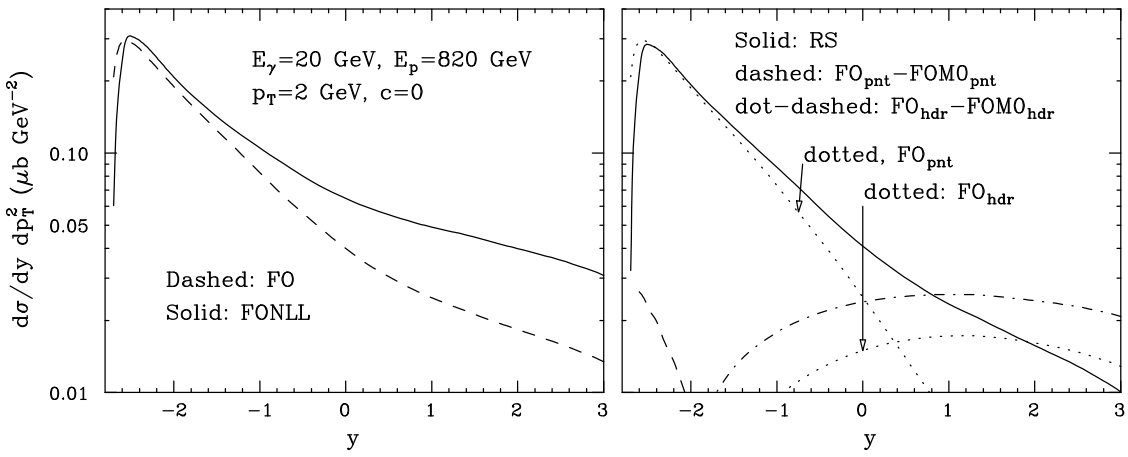

Figure 9: Rapidity distribution of charm quarks at $p_{\rm T} = 2$ GeV, with no smearing factor for the term RS − FOM0 (i.e., $c = 0$). In the right figures the various contributions to the FONLL cross section are shown.

$-2.77 < y < 6.49$. Thus, the left limit of the plots is near the negative rapidity limit. No suppression factor was applied to the difference RS − FOM0. At these low values of $p_{\rm T}$, we would expect that the fixed order and the FONLL result should agree. In fact we observe good agreement at negative rapidity, while at moderate and large rapidity the FONLL result is much larger than the fixed order one.

A detailed analysis of the various contributions to the FONLL cross section is shown in the right plot of the figure. We show the RS result, and the mass corrections FO-FOM0, for the pointlike and hadronic component separately. For comparison, also the fixed order pointlike and hadronic component are shown.

A few comments are in order. We begin by noticing that the difference $\mathrm{FO_{pnt}} - \mathrm{FOM0_{pnt}}$ (the dashed line in the left lower corner of the plot) is quite small compared to $\mathrm{FO_{pnt}}$. On the contrary, $\mathrm{FO_{hdr}} - \mathrm{FOM0_{hdr}}$ is even larger than the $\mathrm{FO_{hdr}}$ result, due to a negative $\mathrm{FOM0_{hdr}}$ contribution. Comparing the pointlike and hadronic fixed order results, we see that the first one prevails up to rapidities of 0.4. A similar plot, for $p_{\rm T} = 3$ GeV, is shown in fig. 10. We see similar features to the case of fig. 9.

We conclude that the large difference between our FONLL and FO results is only due to the hadronic component of the cross section.

This is consistent with what already observed in ref. [12]. In that paper these differences were ascribed to a large RS − FOM0 term which, due to spurious higher

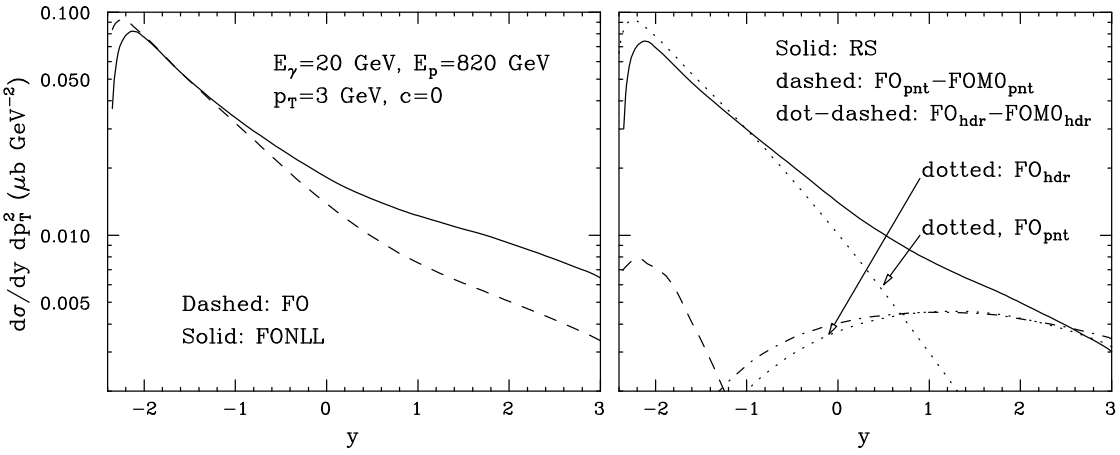

Figure 10: As in fig. 9, for $p_{\rm T} = 3$ GeV.

order terms present in RS, did not vanish quickly enough in the small $p_{\rm T}$ limit. Consequently, the small-$p_{\rm T}$ suppression factor $G(m, p_{\rm T}) = p_{\rm T}^2/(p_{\rm T}^2 + c^2 m^2)$, with $c = 5$, was applied to the difference RS − FOM0 in order to get rid of this problem.

In this work we can now make a conjecture about a possible relation between the higher order behaviour of the "massless" RS calculation and the size of the mass terms: in the hadronic case mass terms are large and so are the higher orders in RS. In the pointlike component, instead, the mass terms are relatively small, and there appears to be a good cancellation between RS and FOM0. One can therefore make the reasonable assumption that the less important the power suppressed mass terms are, the better behaved a resummed "massless" approximation will be.

Having said so, we observe that for the pointlike component alone no suppression factor is actually needed, consistently with what we observed in section 4.

At this point, one is tempted to apply the suppression factor $G(m, p_{\rm T})$ only to the difference $\mathrm{RS_{hdr}} - \mathrm{FOM0_{hdr}}$. However, this would be incorrect. As we have already discussed in section 4, the terms of order $\alpha_{\rm em}\alpha_{\rm s}$ and $\alpha_{\rm em}\alpha_{\rm s}^2$ in $\mathrm{RS_{hdr}}$ do not match $\mathrm{FOM0_{hdr}}$. The difference $\mathrm{RS_{hdr}} - \mathrm{FOM0_{hdr}}$ is of order $\alpha_{\rm em}\alpha_{\rm s}^2$. Thus, using a different c value for the pointlike and hadronic component would lead to the introduction of mass suppressed terms of order $\alpha_{\rm em}\alpha_{\rm s}^2$, that would spoil the accuracy of our calculation. It is instead sensible to use different c values in the following expression

$$\mathrm{FONLL} \;=\; \mathrm{FO_{pnt}} + \mathrm{FO_{hdr}} + (\mathrm{RS_{pnt}} - \mathrm{FOM0_{pnt}} + \mathrm{PQ})\frac{p_{\rm T}^2}{p_{\rm T}^2 + c_{\rm pnt}^2 m^2} +$$

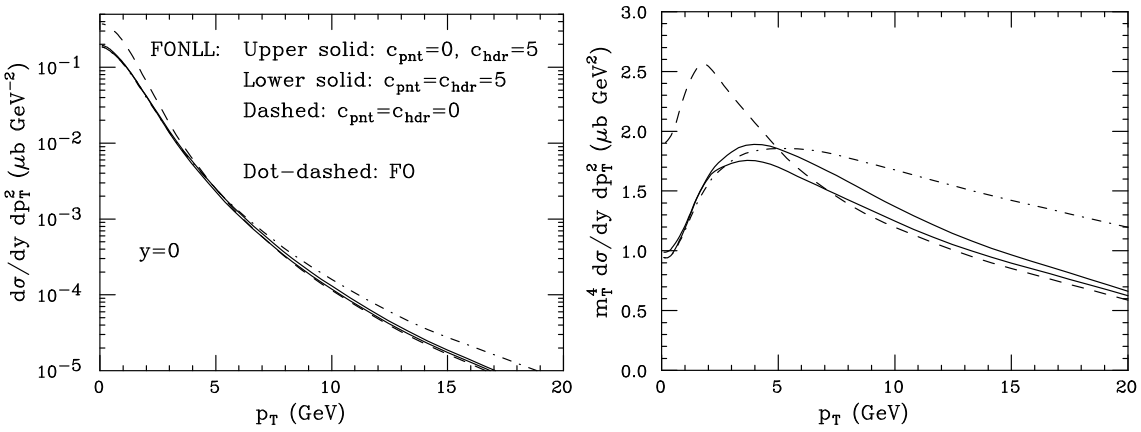

Figure 11: Effect of the smearing functions in the FONLL result (eq. (6.2)) for the $p_{\rm T}$ distribution of charm quarks at $y = 0$. In the right figure, the same results are multiplied by $m_{\rm T}^4$.

$$({\rm RS}_{\rm hdr} - {\rm FOM0}_{\rm hdr} - {\rm PQ}) \frac{p_{\rm T}^2}{p_{\rm T}^2 + c_{\rm hdr}^2 m^2}, \qquad (6.2)$$

since now the expressions in parentheses are indeed of the appropriate order. From formula (6.2) with $c_{\rm pnt} = c_{\rm hdr} = c$ we recover the standard expression eq. (5.2). In fig. 11 we show the effect of varying independently $c_{\rm pnt}$ and $c_{\rm hdr}$ in the FONLL result of eq. (6.2). It is quite clear that the inclusion of a smearing function for the pointlike component has little effect (the difference between the two solid lines). The smearing function for the hadronic component has instead a very large effect, suppressing the cross section at small $p_{\rm T}$. In its absence (dashed curve), one gets a cross section that is roughly twice as large as the fixed order one. At large $p_{\rm T}$ the sensitivity to a smearing function decreases rapidly. The FONLL approach gives smaller cross sections than the fixed order approach in this region. This is what one expects from resummation effects, since the emission of collinear gluons, in general, has the effect of softening the $p_{\rm T}$ spectrum. Similar plots are also shown in fig. 12 for $y = -1$. Also here we see that the effect of the smearing function on the pointlike component of the cross section is small, and we see a relatively large effect of the smearing in the hadronic component. This effect is not quite as large as in the case of $y = 0$, because at negative rapidity the hadronic component is less important.

We shall now show a few benchmark results for photoproduction of heavy flavour at HERA. For simplicity, we shall always keep $c \equiv c_{\rm pnt} = c_{\rm hdr} = 5$. The aim of these results is to assess the difference between the fixed order results, the resummed results,

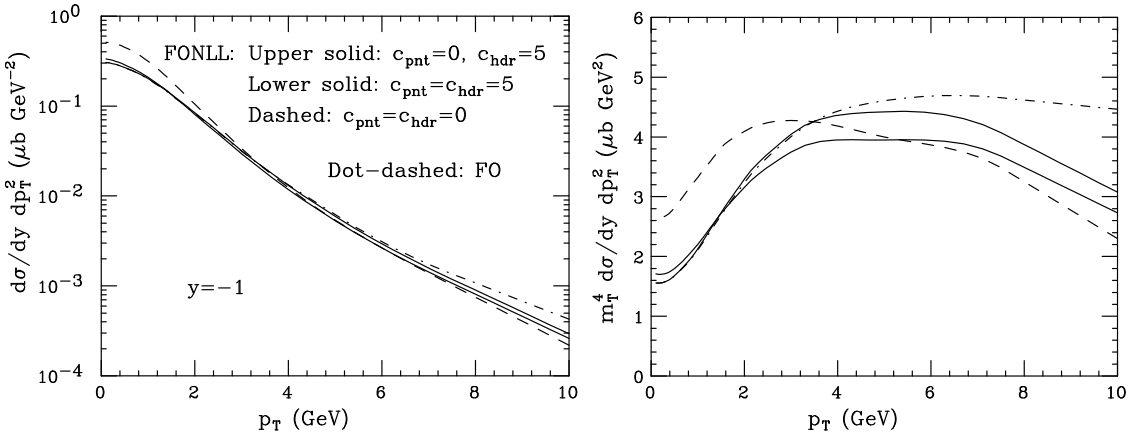

Figure 12: As in fig. 11, for $y = -1$.

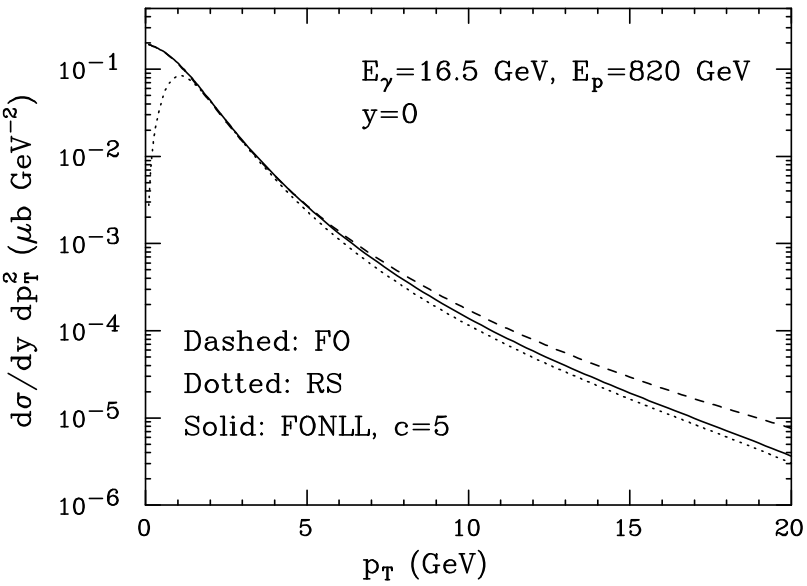

Figure 13: Comparison between the FONLL, FO and RS results.

and our matched formalism. We assume an incident photon energy of 16.5 GeV (corresponding to an electron energy of 27.5 GeV and to a photon energy fraction of 0.6), and a proton energy of 820 GeV. In fig. 13 we show a comparison between the FONLL, FO and RS results. We see that the RS and FO results are remarkably close for small $p_{\rm T}$, a fact that we have understood to be true for the pointlike component, and purely accidental for the hadronic component. At moderate $p_{\rm T}$ also the FONLL result is very close to the FO result. While in the case of the pointlike component

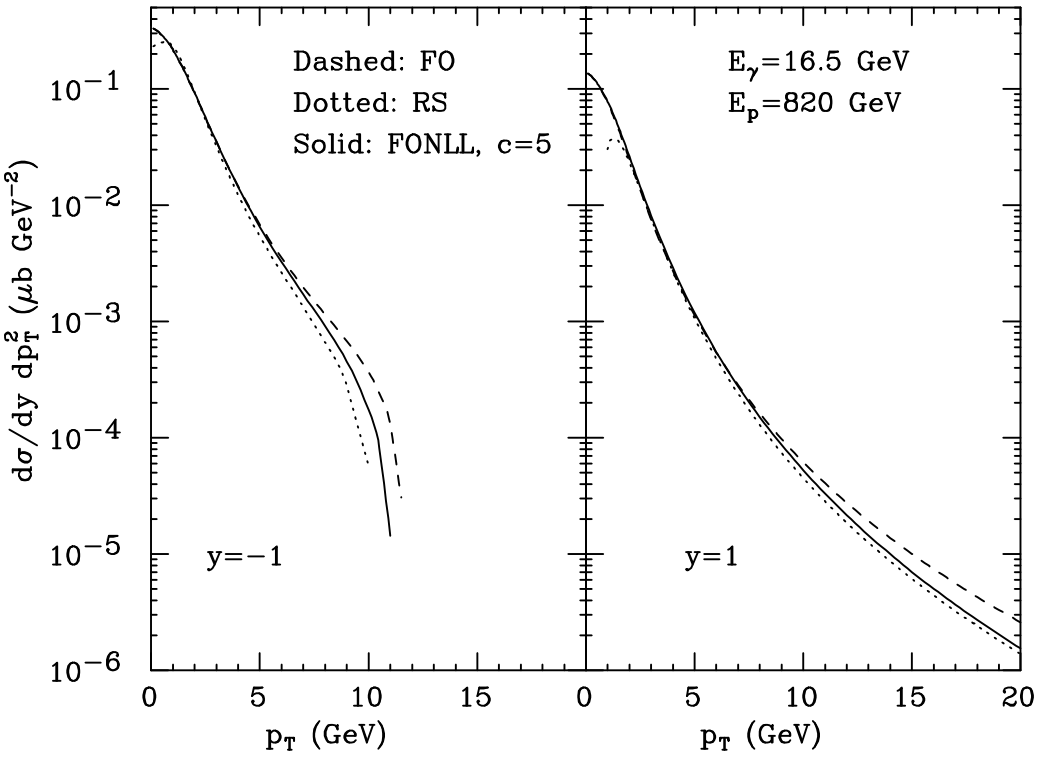

Figure 14: As in fig. 13, for $y = -1$ and $y = 1$.

this is true in all cases, for the hadronic component this only happens if one chooses a relatively large value for c. At very small $p_{\rm T}$ the resummed calculation becomes totally unreliable. At large $p_{\rm T}$, the FONLL and RS results become quite similar (since, by construction, the $G(m, p_{\rm T})$ suppression factor tends to one, and FO tends to FOM0, canceling it - see eqs. (1.11) and (5.2)), and remain smaller than the FO result. This is a general consequence of the effect of multi-gluon emission resummed in the RS and FONLL approaches. The pattern displayed in fig. 13 seems to be quite universal. Similar plots for $y = 1$ and $y = -1$ are shown in fig. 14. Furthermore in fig. 15 we also show the case of photon energy fractions of 0.4 and 0.2 (that is $E_\gamma = 11$ and 5.5 GeV respectively).

7 Conclusions

In this work we have implemented a technique to compute the transverse momentum spectrum in heavy flavour photoproduction, which is accurate to the full NLO

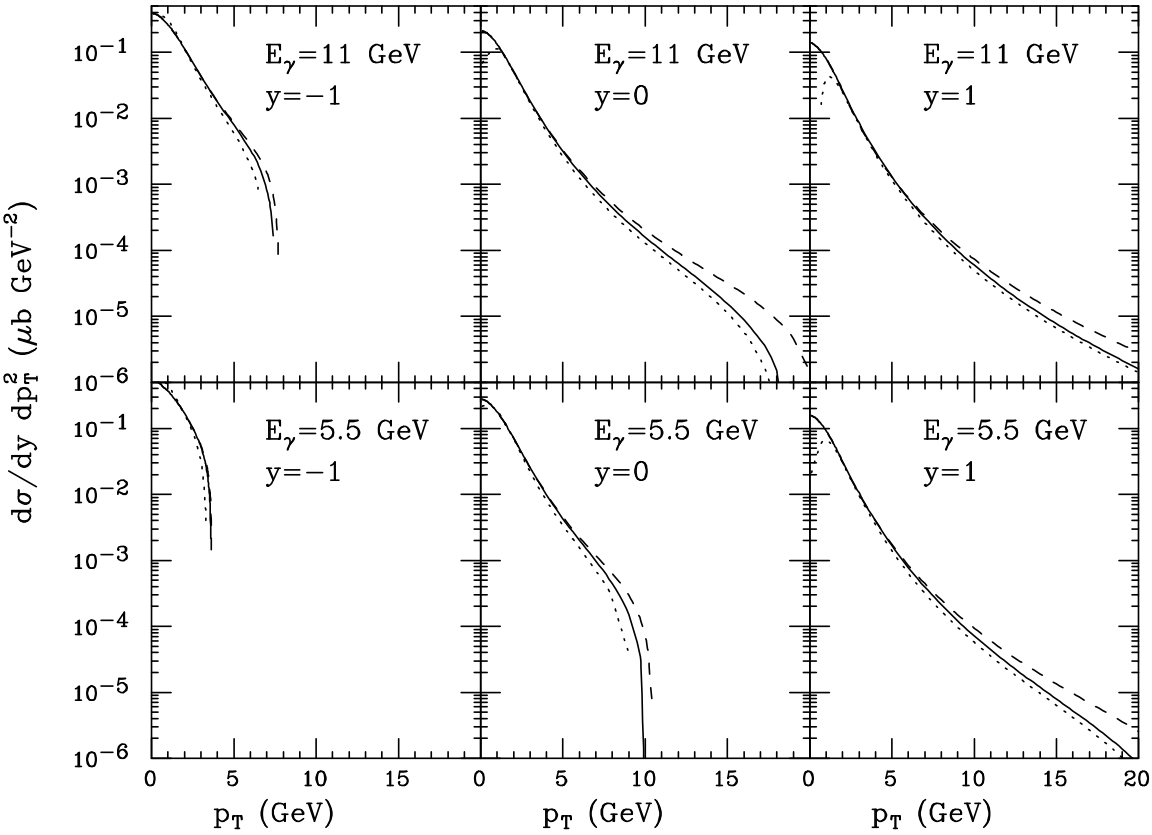

Figure 15: As in figs. 13 and 14, for $E_\gamma = 11$ and 5.5 GeV.

level at moderate $p_{\rm T}$ values, and to the NLL level at large $p_{\rm T}$.

This is achieved by properly merging a "massless" resummed approach, valid in the large-$p_{\rm T}$ region, with a full massive fixed order calculation, reliable in the small-$p_{\rm T}$ one.

We observe that, for the pointlike component of the cross section (in the sense discussed in section 4), the massless limit is a good approximation to the full cross section, provided one uses $m_{\rm T}$ rather than $p_{\rm T}$ in the former. On the contrary, this is not the case for the hadronic component of the cross section, as already observed in ref. [12] in the hadroproduction case: power suppressed mass terms happen to be important in the moderate $p_{\rm T}$ region. This suggests that a proper merging like the one studied in this paper is necessary and superior to just employing a massless approach.

The results obtained with our procedure are in good agreement with the fixed-

order calculations at moderate transverse momenta, and with the so-called massless resummation (or fragmentation function) approach at very large momenta, effectively interpolating, in a theoretically sound manner, between the two approaches.

In general, we find that inclusion of resummation effects brings about a softening of the $p_{\rm T}$ spectrum at large transverse momenta.

Acknowledgments. The authors thank the CERN Theory Division, where much of this work was performed. The work of M.C. was supported in part by the National Science Foundation Contract PHY-9722101.

References

[1] R. K. Ellis and P. Nason, *Nucl. Phys.* **B312**(1989)551.

[2] J. Smith and W.L. Van Neerven, *Nucl. Phys.* **B374**(1992)36.

[3] M. Cacciari and M. Greco, *Z. Phys.* **C69**(1996)459.

[4] B. Mele and P. Nason, *Nucl. Phys.* **B361**(1991)626.

[5] C. Adloff *et al.* [H1 Collaboration], *Nucl. Phys.* **B545**(1999)21.

[6] J. Breitweg *et al.* [ZEUS Collaboration], *Eur. Phys. J.* **C6**(1999)67.

[7] P. Nason, S. Dawson and R. K. Ellis, *Nucl. Phys.* **B303**(1988)607.

[8] P. Nason, S. Dawson and R. K. Ellis, *Nucl. Phys.* **B327**(1989)49; erratum *ibid.* **B335**(1990)260.

[9] W. Beenakker, H. Kuijf, W.L. van Neerven and J. Smith, *Phys. Rev.* **D40**(1989)54.

[10] W. Beenakker, W.L. van Neerven, R. Meng, G.A. Schuler and J. Smith, *Nucl. Phys.* **B351**(1991)507.

[11] M. Cacciari and M. Greco, *Nucl. Phys.* **B421**(1994)530, `hep-ph/9311260`.

[12] M. Cacciari, M. Greco and P. Nason, JHEP05(1998)007, `hep-ph/9803400`.

[13] F. Aversa, M. Greco, P. Chiappetta and J. P. Guillet, *Z. Phys.* **C46**(1990)253.

[14] P. Aurenche, R. Baier, A. Douiri, M. Fontannaz and D. Schiff, *Nucl. Phys.* **B286**(1987)553.

[15] H.L. Lai *et al.*, *Phys. Rev.* **D55**(1997)1280, `hep-ph/9606399`.

[16] J.C. Collins and Wu-Ki Tung, *Nucl. Phys.* **B278**(1986)934.

[17] P. Aurenche, J.P. Guillet and M. Fontannaz, *Z. Phys.* **C64**(1994)621.